VII International Conference on Particle-Based Methods
PARTICLES2021
P. Wriggers, M. Bischoff, E. Oñate, A. Düster& T. Zohdi(Eds)

PFEM ANALYSIS OF INSTALLATION EFFECTS ON AXIAL PERFORMANCE OF JACKED PILES IN CHALK

MATTEOO. CIANTIA[*], JIANGTAO LEI[†], LLUIS MONFORTE[°], MARCOS ARROYO[†] AND ANTONIOGENS[†]

[*] School of Science and Engineering, University of Dundee
Nethergate DD1 4HN, Dundee Scotland, UK
e-mail: m.o.ciantia@dundee.ac.uk, https://www.dundee.ac.uk/

[†]UniversidadPolitècnica de Catalunya (UPC)
Campus Norte UPC, 08034 Barcelona, Spain
e-mail: jiangtao.lei@upc.edu, https://www.upc.edu/ca

[°]Centre Internacional de MètodesNumèrics en Enginyeria (CIMNE)
Campus Norte UPC, 08034 Barcelona, Spain
e-mail: lmonforte@cimne.upc.edu, https://www.cimne.com

Key words: Chalk, GPFEM, Monopiles, Installationeffects.

Abstract. Chalk covers areas of the UK and is widespread under the North and Baltic Seas where OWT are currently being installed and where future offshore expansion will be sited. Large piles are often driven in chalk to support OWT and other onshore infrastructure. The installation of pile foundations causes the intact rock surrounding the pile to crush and deteriorates into a putty characterised by a mechanical behaviour very different from the intact chalk. Such complexity is the underlying reason for inadequate current design guidance for pile in chalk which currently relies on empirical methods or partial (wished-in-place) numerical simulations. Installation effects such as grain crushing and pore pressure generation are conservatively estimated (if considered at all), as the change of rock properties around the pile during the installation process cannot be easily quantified. In this paper it is shown how advanced numerical modelling can be used to capture such damaging effects and hence guide the design of pile foundations in chalk. The coupled hydro-mechanical effects developing during pile installation are investigated numerically using a robust and mesh-independent implementation of an elasto-plastic constitutive model for chalk recently reformulated in large strains. The model implemented into an open source Particle Finite Element (PFEM) code, is able to capture the damage of the rock until the formation of a chalk putty layer around the shaft of a small diameter pile. Installation effects are highlighted by comparing the axial performance between wished in place piles and piles which considered the full installation process. The numerical results are then used to critically address the limitation of current design specifications of displacement piles in chalk.

1 INTRODUCTION

Chalk covers much of the UK and is widespread under the North and Baltic Seas where many offshore wind turbines (OWT) are currently being installed and where future offshore deployment will be hosted. Large piles are often driven in chalk to support OWT and other onshore infrastructure. Dynamic installation of pile foundations in chalk causes extremely high pore-water pressure (*pwp*) build up, the intact rock surrounding the pile to crush and deteriorate into chalk putty which is characterised by a mechanical behaviour completely different from the initial intact chalk[1]. Such complexity is the underlying reason for inadequate current design guidance for pile driveability, axial and lateral static load response [2]. The long-term performance in service as well as cyclic loading performance remain highly significant unknowns, making pile design likely overconservative. Considering that for OWT, foundations account for about 20-25% of the total development cost [3], pile design improvements in complex ground as chalk is, can be extremely beneficial from an economical and environmental perspective. Current guidelines for the design of driven piles in chalk (CIRIA C574) originate from the analysis of a limited number of pile tests [1]. These guidelines suggest crude average ultimate unit shaft friction (τ_{sf}) design values of between 20 and 120 kPa for sites where low-medium density and high very-high density chalk is present, respectively. These shaft friction estimates are thought to be conservative and to introduce significant increases in cost and carbon footprint. Even less guidance is available regarding cyclic or lateral loading in chalk, although this is often crucial in offshore pile design. Pile installation crushes the chalk and produces an annulus of 'putty chalk' around the pile [4,5]. The pile in-service performance relies on both stiffness and strength of this putty (τ_{sf}) and the post installation stress state around the pile. Recent field tests[6,7] have also shown that τ_{sf} can increase significantly with time post installation (set-up of up to 400% over a few months). However, such set-up was not observed when smaller piles were slowly jacked into the ground. This clearly indicates that installation effects play a major role in the in-service performance. Moreover, these time dependent phenomena appear to be site specific and, despite the large number of time consuming and expensive field tests performed, the mechanisms explaining this complex behaviour are not yet completely understood. In this paper the pile installation process is investigated through large deformation numerical analyses with a finite deformation plasticity model for structured sands to model the chalk. Installation effects are highlighted by comparing the axial performance between wished in place piles and piles which considered the full installation process. The numerical results are then used to critically address the limitation of current design specifications of displacement piles in chalk.

2 CONSTITUTIVE MODEL FOR CHALK

Soft rock behaviour can be mathematically described by extending the strain hardening plasticity framework used to model soils by increasing the size of the yield locus giving the material tensile strength [8]. In particular the intersections of the yield locus ($f = 0$) with the positive and negative p' axis are called $p_c = p_s + p_m$, and p_t; p_s acts as preconsolidation pressure, as it is for soils, and it is assumed to depend on both plastic volumetric and deviatoric strain rates. In contrast, p_t and p_m account for the effects of interparticle bonding (Figure 2). The existence of bonds therefore implies a non-zero tensile strength (p_t> 0) and an increase in the yield stress along radial loading paths [9]. $p_m$corresponds to this increase in the case of isotropic compression path.

The constitutive model has been formulated in the framework of large strains elasto-plasticity with a multiplicative decomposition of the deformation gradient into elastic and plastic parts [10]. This framework ensures that rigid body motions of the deformable body do not produce spurious stress variations (frame indifference) and also that energy is preserved since a hyper-elastic model is employed. In this work the shape of the yield envelope is built around the Modified Cam Clay model. The yield surface is hence defined as:

$$f(\boldsymbol{\tau}', p_s, p_t, p_m) = \left(\frac{q}{M}\right)^2 + p^*(p^* - p_c^*) \tag{1}$$

where $q = \sqrt{3J_2}$ and J_2 is the second invariant of the effective Kirchoff stress tensor, $\boldsymbol{\tau}'$. M is the slope of the Critical state line in the $p' - q$ plane whereas:

$$p^* = p' + p_t \tag{2}$$

$$p_c^* = p_t + p_s + p_m \tag{3}$$

where $p' = \ tr(\boldsymbol{\tau}')\ /3$ is the first invariant of the Kirchoff stress tensor. The yield locus in the triaxial plane is depicted in Figure 1; that also graphically defines the plastic stress-like variables p_c^*, p_t, p_s and p_m. On the one hand, p_s is the preconsolidation pressure of the reference, unstructured soil (putty). On the other hand, p_t and p_m account for the effect of structure: p_m corresponds to the increase in the yield stress along isotropic compression paths whereas p_t is the tensile strength. Generally, these two hardening variables are considered to be proportional [11], being *c* the proportionality factor:

$$p_t = cp_m \tag{4}$$

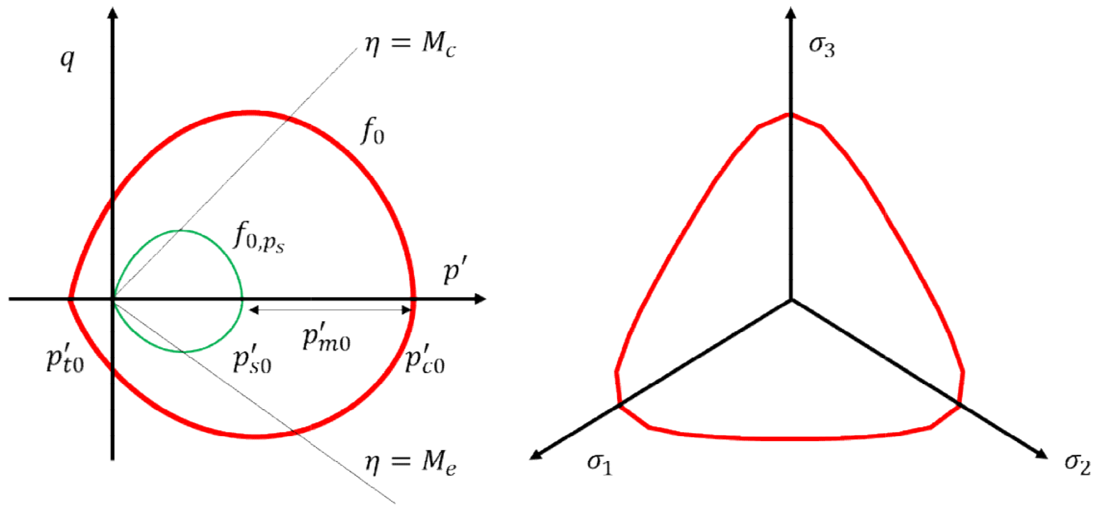

Figure 1: Yield surface in the triaxial (left) and deviatoric (right) planes

The evolution of the hardening variables is related to the plastic volumetric and distortional flow:

$$\dot{p_s} = \rho_s p_s \left(tr(\boldsymbol{l}^p) + \chi_s \sqrt{\frac{2}{3}} \|dev(\boldsymbol{l}^p)\| \right) \tag{5}$$

$$\dot{p_t} = -\rho_t p_t \left(|tr(\boldsymbol{l}^p)| + \chi_s \sqrt{\frac{2}{3}} \|dev(\boldsymbol{l}^p)\| \right) \tag{6}$$

where ρ_s, χ_s, ρ_t and $\chi_s$are constitutive parameters and $\boldsymbol{l}^p$ is the spatial plastic velocity gradient. The elastic response is characterized by means of an hyperelastic model incorporating a tensile range [12], which is formulated in terms of the Hencky strain and the Kirchhoff stress tensor. For further details of the constitutive model refer to [13,14].

2.1 Nonlocal integration

A nonlocal integral type regularization technique is used to mitigate the pathological mesh-dependence that exhibit numerical simulations where softening is encountered. As such, the expression of a nonlocal variable $\tilde{\beta}$ is:

$$\tilde{\beta}(\boldsymbol{x}) = \frac{\int_{\Omega} w(\boldsymbol{x}, \|\boldsymbol{x}-\boldsymbol{y}\|)\beta(\boldsymbol{y})\, d\Omega}{\int_{\Omega} w(\boldsymbol{x}, \|\boldsymbol{x}-\boldsymbol{y}\|)\, d\Omega} \tag{7}$$

where $w(\boldsymbol{x}, \|\boldsymbol{x}-\boldsymbol{y}\|)$ is the weighting function for point $\boldsymbol{x}$ controlling the influence of its neighbors in terms of their relative distance. In this work, plastic strains are considered as nonlocal variables; from these values $p_s$and p_t may be obtained by integrating analytically equations (5) and (6). The weighting function proposed by [15] is employed here as it has been found to outperform other weighting functions in removing mesh bias.

2.1 Model parameters

Given a set of uniaxial compressive strength (UCS) and or triaxial compression experimental data it is possible to calibrate the model following a procedure described by[16]. The goal here is to show the potential of the numerical approach, hence the constitutive parameters have been chosen to represent a generic intact chalk with a UCS of 290 kPa, Young modulus of 100 MPa and Poisson ratio of 0.2. The values of the constitutive parameters are reported in Table 1. Figure 2 reports the results (the effective stress path and the load-displacement curve) of drained and undrained triaxial compression tests at two levels of confinement pressures. As clearly represented in the figure once the stress path reaches the yield surface, destructuration begins and for the low confinement tests deviatoric stresses decrease until the critical state is reached. For the highly confined tests, after the peak and an initial softening phase the deviatoric stress increases until the same critical state is reached. Complete destructuration is reached when p_t (hence tensile strength) goes to zero. For more details of the behavior of the chalk putty (unbonded state) refer to [8].

Table 1: Constitutive parameters adopted in this work for a generic intact chalk

E (kPa)	ν	M	p_s (kPa)	p_t (kPa)	ρ_s	ρ_t	χ_s	χ_t	c	k (m/s)
100000	0.2	1.5	150	50	12.9	8	0	0.5	4	10^{-5}

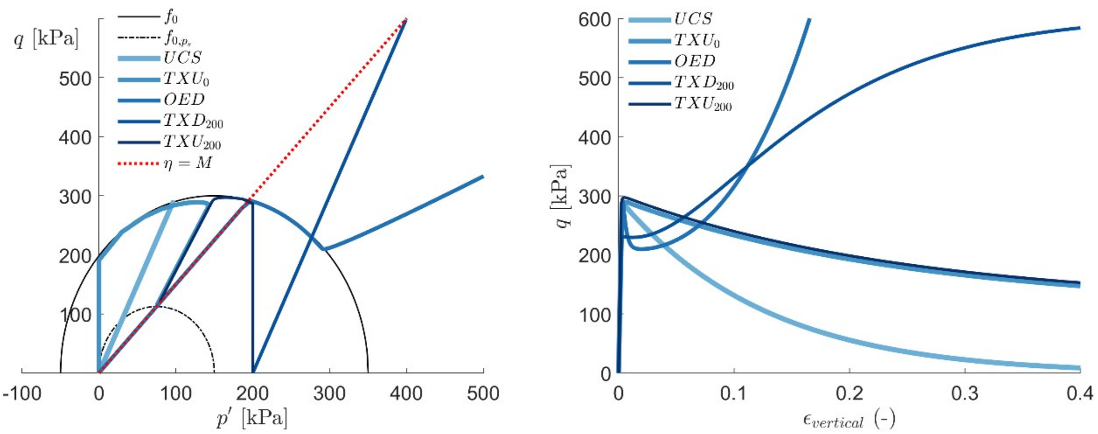

Figure 2: UCS, oedometric compression, drained and undrained triaxial response in the p'-q plane (left) and corresponding evolution of deviatoric stresses in terms of the axial deformation (right)

3 NUMERICAL SIMULATION OF PILE INSTALLATION

The model is implemented in the open source [17] platform KRATOS (*https://www.cimne.com/kratos/default.asp*).We simulate the penetration of a rough -friction μ=0.2 - cone-tipped model pile of 3.6 cm diameter. Geometry. initial conditions and initial mesh are represented in Figure 3. To investigate the effect of installation on the axial capacity the following set of simulations are run. Two *wished-in-place* (WIP) piles are numerically tested in tension and compression. Their response will not be affected byany installation effect. Two *fully installed piles* (FIP) are tested in tension and compression. In these simulations, after the pile is installed until the same penetration depth of the WIP models, the excess pore water pressures are left to dissipate before testing the pile in tension and compression respectively.

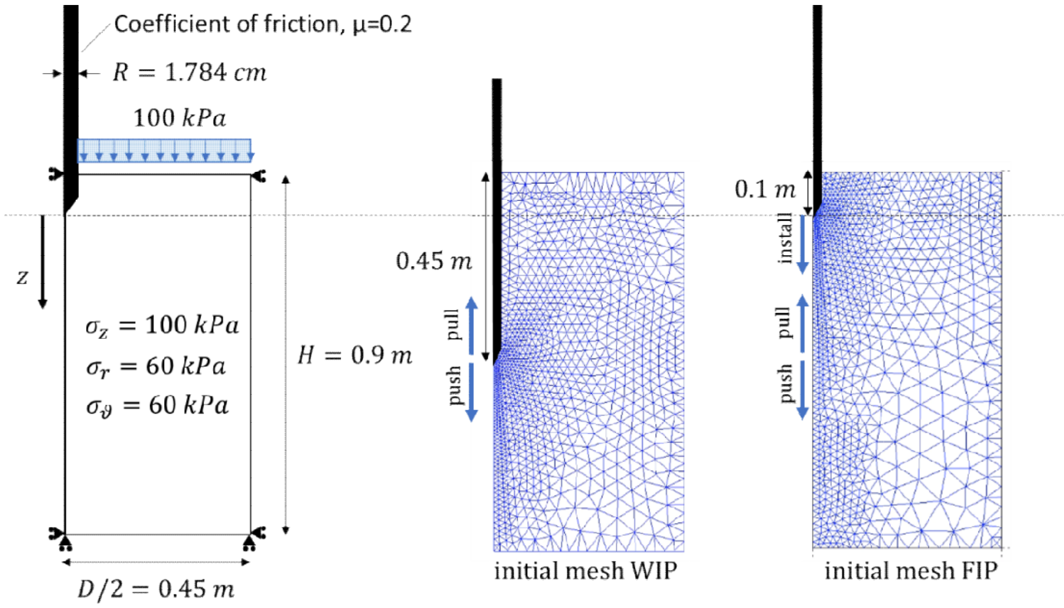

Figure 3: Calibration chamber geometry and initial conditions

From the WIP initial condition the tensile capacity of the pile is tested by extracting the pile at a constant velocity of 0.02 m/s on the other hand the compressive capacity is determined by pushing the pile downwards. These two simulations are represented in Figure 4 and are represented by the lines that go from point X to points Y and Z respectively. The FIP are first jacked into the ground at a velocity of 0.02 m/s until the same penetration depth of the WIP models is reached (from point A to point B). At this point the pile is unladed until the vertical force is zero (point C). At this point, after a dissipation phase of 100 days, the pile is either pushed down at 0.02 m/s until point D to determine the compressive axial capacity of the FIP model. On the other hand, the pile is extracted at a velocity of 0.02 m/s up to point E to determine the tensile capacity of the FIP. The results clearly show that installation effects have a big influence on the axial capacity. Despite the chalk is crushed into a cohesionless material (chalk-putty), the increase of confinement around the pile is responsible of an increase of both tensile and compression capacity. The tensile capacity is more than doubled while the compressive capacity increases by 35%. The model also shows a stiffer response of the FIP models.

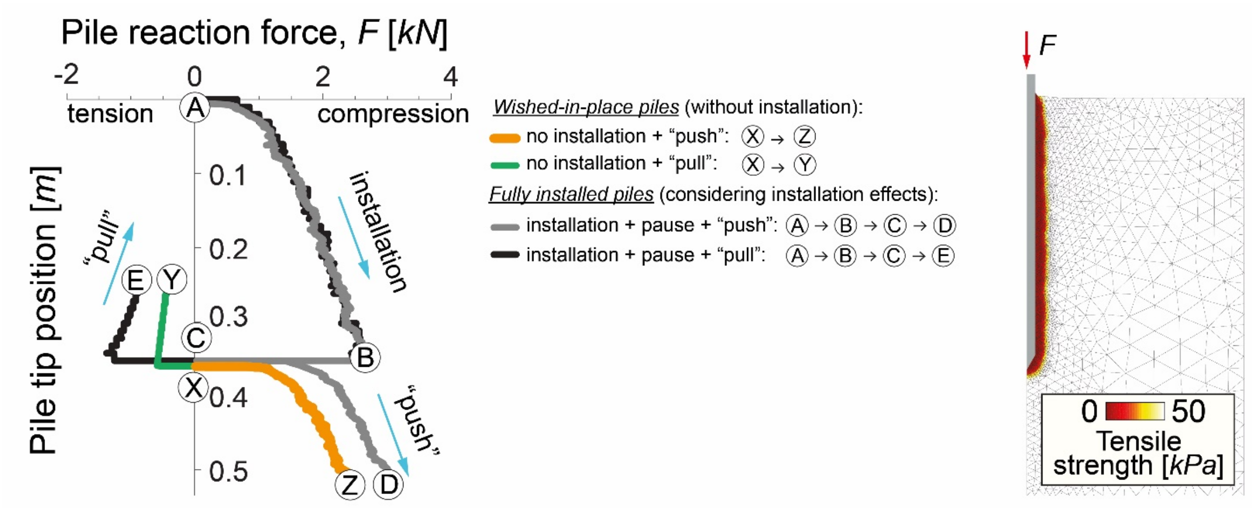

Figure 4: Comparison of the WIP and FIP models in terms of axial response and degradation

4 CONCLUSIONS

This paper shows how advanced numerical modelling can be used to guide the design of the foundations in soft rocks – cemented sands such as chalk. The coupled hydro-mechanical installation effects of pile jacking were addressed numerically using a recently developed constitutive model for soft rocks implemented in an open-source Particle Finite Element Method (PFEM) platform. Installation effects on pile performance are highlighted by comparing the axial capacity between wished in place piles (WIP) and piles which considered the full installation process (FIP). The results show that, there is a competing effect between the installation induced stress increase and rock degradation. The former is responsible for an increased confinement of the pile whilst the latter a decrease of mechanical strength of the reacting soil. The results show that tensile and compression capacity doubled and increased by 35% respectively because of installation effects. Further research is required to better investigate such behaviour considering larger diameter piles, less permeable conditions and -or impact driving loading.

REFERENCES

[1] Lord JA, Clayton CRI, Mortimore RN, Construction Industry Research and Information Association. Engineering in chalk. CIRIA; 2002.

[2] Jardine RJ. Geotechnics, energy and climate change: the 56th Rankine Lecture. Géotechnique 2019:1–57. doi:10.1680/jgeot.18.rl.001.

[3] Ng C, Ran L. Offshore wind farms: Technologies, design and operation. Elsevier Inc.; 2016. doi:10.1016/C2014-0-00763-0.

[4] Alvarez Borges FJ. The shaft capacity of small displacement piles in chalk 2019.

[5] Alvarez-Borges F, Ahmed S, Madhusudhan BN, Richards D. Investigation of pile penetration in calcareous soft rock using X-ray computed tomography. Int J Phys Model Geotech 2021:1–15. doi:10.1680/jphmg.20.00031.

[6] Buckley RM, Jardine RJ, Kontoe S, Parker D, Schroeder FC. Ageing and cyclic behaviour of axially loaded piles driven in chalk. Géotechnique 2017:1–16. doi:10.1680/jgeot.17.P.012.

[7] Ciavaglia F, Carey J, Diambra A. Monotonic and cyclic lateral tests on driven piles in Chalk. Proc Inst Civ Eng - Geotech Eng 2017;170:353–66. doi:10.1680/jgeen.16.00113.
[8] Ciantia MO, di Prisco C. Extension of plasticity theory to debonding, grain dissolution, and chemical damage of calcarenites. Int J Numer Anal Methods Geomech 2016;40:315–43. doi:10.1002/nag.2397.
[9] Ciantia MO, Castellanza R, di Prisco C. Experimental Study on the Water-Induced Weakening of Calcarenites. Rock Mech Rock Eng 2015;48:441–61. doi:10.1007/s00603-014-0603-z.
[10] Simo JC (Juan C., Hughes TJR. Computational inelasticity. New York: Springer; 1998.
[11] Ciantia MO. A constitutive model for the hydro-chemo-mechanical behaviour of chalk. Eng. Chalk, ICE Publishing; 2018, p. 275–81. doi:10.1680/eiccf.64072.275.
[12] Tamagnini C, Ciantia MO. Plasticity with generalized hardening: Constitutive modeling and computational aspects. Acta Geotech 2016;11. doi:10.1007/s11440-016-0438-8.
[13] Monforte L, Ciantia MO, Carbonell JM, Arroyo M, Gens A. A stable mesh-independent approach for numerical modelling of structured soils at large strains. Comput Geotech 2019;116:103215. doi:10.1016/j.compgeo.2019.103215.
[14] Oliynyk K, Ciantia MO, Tamagnini C. A finite deformation multiplicative plasticity model with non – local hardening for bonded geomaterials. Comput Geotech 2021.
[15] Galavi V, Schweiger HF. Nonlocal multilaminate model for strain softening analysis. Int J Geomech 2010;10:30–44. doi:10.1061/(ASCE)1532-3641(2010)10:1(30).
[16] Rios S, Ciantia M, Gonzalez N, Arroyo M, da Fonseca AV. Simplifying calibration of bonded elasto-plastic models. Comput Geotech 2016;73. doi:10.1016/j.compgeo.2015.11.019.
[17] Oñate E, Idelsohn SR, del Pin F, Aubry R. The particle finite element method – an overview. Int J Comput Methods 2004;01:267–307. doi:10.1142/s0219876204000204.
[18] https://www.cimne.com/kratos/default.asp n.d.